

1 **Developing efficient structural systems for small satellites**

2 Shubhankar Sinha¹, Arivarasu M¹

3 ¹School of Mechanical Engineering, Vellore Institute of Technology (VIT), Vellore 632014, Tamil Nadu, India

4 **ABSTRACT**

5 The growing demand for small satellites, including CubeSats and nanosatellites, is reshaping the space industry
6 by offering affordable, versatile, and rapidly deployable solutions for Earth observation, communications, and
7 scientific missions. Despite these advantages, their compact form presents significant engineering challenges—
8 particularly in developing structural systems that are both lightweight and capable of withstanding the stresses of
9 launch and the extreme conditions of space. Tackling these issues is essential to improve mission reliability and
10 long-term sustainability.

11 This study aims to develop structural designs that minimize weight while preserving mechanical strength and
12 load-bearing performance. It utilizes advanced optimization techniques, such as topology optimization and genetic
13 algorithms, to generate innovative and efficient structural solutions. The research also investigates iso-grid and
14 honeycomb structures, known for their excellent strength-to-weight ratios and compatibility with modern
15 fabrication methods.

16 Additive Manufacturing (AM) commonly known as 3D printing—is central to this approach. It enables the
17 creation of complex geometries and customized components that traditional manufacturing methods cannot easily
18 produce. AM not only supports material-efficient designs but also allows for rapid prototyping and cost-effective
19 production, making it especially suitable for small satellite development. Combining AM with iso-grid and
20 honeycomb structures further enhances design flexibility for various mission profiles.

21 In summary, this work presents a comprehensive framework for designing efficient and sustainable structural
22 systems for small satellites. The outcomes are expected to boost mission efficiency, increase accessibility, and
23 drive innovation in satellite engineering in response to the growing needs of the space sector.

24 **Keywords:** *CubeSats; iso-grid; honeycomb; additive manufacturing; 3D printing*

25 **1 Introduction**

26 The small satellite industry, particularly CubeSats and nanosatellites, has transformed space accessibility over the
27 past decade. These compact platforms enable diverse missions—from Earth observation and communications to
28 scientific experiments—at a fraction of traditional satellite costs. By lowering financial and technical barriers,
29 small satellites have democratized space access, enabling universities, commercial startups, and emerging space
30 nations to participate in orbital operations and drive innovation in the sector.

31 However, miniaturization introduces significant engineering challenges. Limited physical volume creates
32 competing demands: structures must be lightweight to reduce launch costs, yet mechanically robust enough to
33 survive harsh launch environments and operational conditions. In aerospace systems, mass directly correlates with
34 mission economics—each additional kilogram substantially increases propellant requirements and launch
35 expenditure. Structural designers must therefore optimize mass while maintaining sufficient strength, stiffness,
36 and reliability throughout the mission lifecycle.

37 This research addresses the mass-strength paradox through the development of structurally optimized small
38 satellite platforms. The primary objective is designing lightweight structures capable of withstanding launch-
39 induced vibrations, mechanical shocks, and on-orbit thermal cycling, while remaining cost-effective to
40 manufacture and adaptable across mission profiles. The approach integrates computational optimization methods
41 with Additive Manufacturing (AM) technologies to achieve performance targets unattainable through
42 conventional fabrication techniques.

43 Additive Manufacturing has fundamentally disrupted aerospace component production. Traditional subtractive
44 methods—machining, casting, forging—impose geometric constraints and generate substantial material waste.
45 These processes typically yield conservative designs with excess mass to ensure safety margins. Conversely, AM's
46 layer-by-layer deposition enables fabrication of complex geometries previously considered unmanufacturable,
47 including internal lattice networks, conformal cooling channels, and functionally graded materials. This design
48 freedom allows structures to be tailored precisely to their loading conditions.

49 The research employs topology optimization as its primary design strategy. This computational method iteratively
50 removes material from a design domain while maintaining structural performance under specified loads. The
51 algorithm identifies optimal load paths and material distribution, producing organic, biomimetic forms that
52 maximize stiffness-to-weight ratios. For small satellites, topology optimization can reduce structural mass by 30-
53 50% compared to conventional designs without compromising mechanical integrity.

54 Complementing topology optimization, the study implements genetic algorithms for multi-objective design
55 exploration. These evolutionary computation techniques generate populations of candidate designs and improve
56 them through selection, crossover, and mutation operations mimicking biological evolution. Genetic algorithms
57 excel at navigating complex design spaces with competing objectives—simultaneously minimizing mass while
58 maximizing natural frequency and factor of safety. Their probabilistic nature enables discovery of non-intuitive
59 solutions that gradient-based methods might overlook.

60 The structural design incorporates three high-performance geometric patterns: lattice structures, isogrids, and
61 honeycomb cores. Lattice structures feature periodic networks of thin struts providing exceptional stiffness per
62 unit mass. Isogrid reinforcement patterns—characterized by triangular stiffening ribs—deliver quasi-isotropic
63 mechanical properties ideal for cylindrical and planar components. Honeycomb architectures offer outstanding
64 compressive strength and energy absorption through their cellular geometry. All three configurations leverage
65 AM's capability to produce intricate internal features impossible with conventional manufacturing.

66 Material selection considers mission-specific thermal, mechanical, and electromagnetic requirements. Titanium
67 alloys (Ti-6Al-4V) provide high strength and corrosion resistance for demanding applications. Aluminium alloys
68 (AlSi10Mg) offer favourable strength-to-weight ratios and thermal conductivity for general-purpose structures.
69 High-performance polymers enable rapid prototyping and specialized applications requiring electromagnetic
70 transparency. Manufacturing utilizes Selective Laser Melting (SLM) for metallic components and Fused
71 Deposition Modelling (FDM) for polymer structures.

72 Design validation combines computational simulation with physical testing. Finite Element Analysis (FEA)
73 predicts structural response under launch vibrations (quasi-static loads up to 10g), random vibration profiles,
74 acoustic loads, and thermal extremes (-150°C to +120°C). Simulations identify stress concentrations and verify
75 adequate safety factors before fabrication. Subsequently, AM-produced prototypes undergo qualification testing—
76 random vibration tests per NASA-GEVS standards, thermal vacuum cycling, and mechanical load testing—to
77 demonstrate flight readiness.

78 Anticipated outcomes include 40-60% mass reduction compared to traditionally manufactured equivalents,
79 improved stress distribution eliminating localized failure modes, and enhanced platform modularity. These
80 advances translate directly to mission value: increased payload capacity, extended operational lifetime through
81 reduced structural fatigue, and decreased launch costs enabling more frequent missions. Additionally, AM's rapid
82 iteration capability compresses development timelines from months to weeks, accelerating technology maturation
83 and market responsiveness.

84 The research contributes to sustainable space operations through resource-efficient design and manufacturing.
85 Lightweight structures require less raw material extraction and processing energy. Reduced launch mass decreases
86 propellant consumption and associated emissions. AM's near-net-shape production minimizes material waste
87 compared to subtractive machining that discards 70-90% of stock material. Furthermore, distributed AM
88 manufacturing enables regional production, reducing transportation-related environmental impacts and supply
89 chain vulnerabilities.

90 This study advances small satellite structural engineering by utilizing computational optimization with additive
91 manufacturing techniques. The methodology produces application-specific designs that uses AM's geometric
92 freedom while maintaining aerospace qualification standards. Beyond immediate CubeSat applications, the
93 techniques developed here inform future spacecraft design paradigms. As satellite constellations proliferate and
94 missions diversify, such optimization-driven approaches become essential for economically viable and
95 environmentally responsible space systems.

96 **2 Research Methods**

97 **2.1 Design, Verification, and Fabrication**

98 The Design and Analysis included developing conceptual and detailed models of the satellite chassis using
99 honeycomb and isogrid configurations in CAD software. These designs were chosen for their strength-to-weight

100 ratios in aerospace applications. Further, they were refined to incorporate internal compartments for subsystem
101 placement and standardized mounting interfaces for future operations.

102 Finite Element Analysis (FEA) was employed to assess the mechanical performance of these designs under
103 simulated space launch conditions, including vibration, acceleration, and thermal expansion. This simulation-
104 driven process allowed for the iterative refinement of material layout and structural reinforcements to mitigate
105 stress concentrations.

106 During the Verification and Comparison phase, the performance of the isogrid and honeycomb models was
107 documented and compared based on critical performance indicators: weight, maximum stress experienced, factor
108 of safety (FoS), and natural frequency. While honeycomb structures generally demonstrated superior performance
109 in evenly distributing loads, isogrid structures excelled under localized point loads. This comparative analysis
110 determined the optimal structure based on the intended mission profile, while also verifying the design's
111 practicality for manufacturability.

112 The project further employed fabrication using AM, specifically the Fused Deposition Modelling (FDM)
113 technique. FDM was selected for its cost-effectiveness and capacity to produce complex structural components
114 using space-compatible thermoplastic filaments. Functional features such as wire routing paths and component
115 mounts were directly integrated during the printing process, reducing the need for secondary manufacturing and
116 post-assembly work.

117 **2.2 Analysis and Simulation Objectives**

118 The structural development of small satellites is guided by the necessity to ensure a precise and innovative
119 framework under stringent constraints. The key objectives guiding the development and analysis are summarized
120 in **Table 1**.

121 **Table 1:** Analysis and Simulation Objectives

Objective	Rationale and Significance	Design Approach
Mass Efficiency	Minimizing structural mass maximizes payload capacity and reduces launch costs.	Use of advanced lightweight materials (e.g., carbon fibre composites) and Topology Optimization via FEA.
Modularity & Scalability	Enables easy reconfiguration for diverse missions and future capability expansion.	Development of standardized, compartmentalized modules with common, interchangeable interfaces.
Manufacturing	Allows for rapid prototyping, customization, and efficient mass reduction of complex geometries.	Utilization of Additive Manufacturing (AM) with space-grade materials (e.g., Aluminium 7075) and integrated feature printing.
Integration	Ensures the structure accommodates and supports all subsystems (power, propulsion, payload).	Design of flexible mounting platforms, vibration isolation techniques, and integrated cooling/wiring pathways.
Thermal Management	Facilitates passive heat control, critical for satellites lacking active thermal systems.	Integration of heat sinks, radiative surfaces, and use of thermally conductive materials or phase-change materials.
Reliability	Guarantees endurance under extreme launch loads and the orbital environment.	Thorough FEA, conservative safety margins ($\text{FoS} > 1.5$), and use of shock-absorbing joints.
Sustainability	Minimizes space debris in alignment with environmental concerns.	Design for complete deorbit within the mission lifetime and incorporation of deorbiting mechanisms.

123 **2.3 Finite element analysis**

124 The structural performance was analysed using Ansys 2025R1 Student Version. The simulation study focused on
125 static structural analysis to evaluate the design's strength against the axial, lateral, and torsional forces encountered
126 during launch.

127 The simulation setup defined boundary conditions, mimicking the attachment of the satellite structure to the
128 launch vehicle by applying fixed constraints at the mounting interfaces. External forces were introduced to
129 simulate the intense dynamic loads, acceleration, and vibrational frequencies characteristic of a Low-Earth Orbit
130 launch mission.

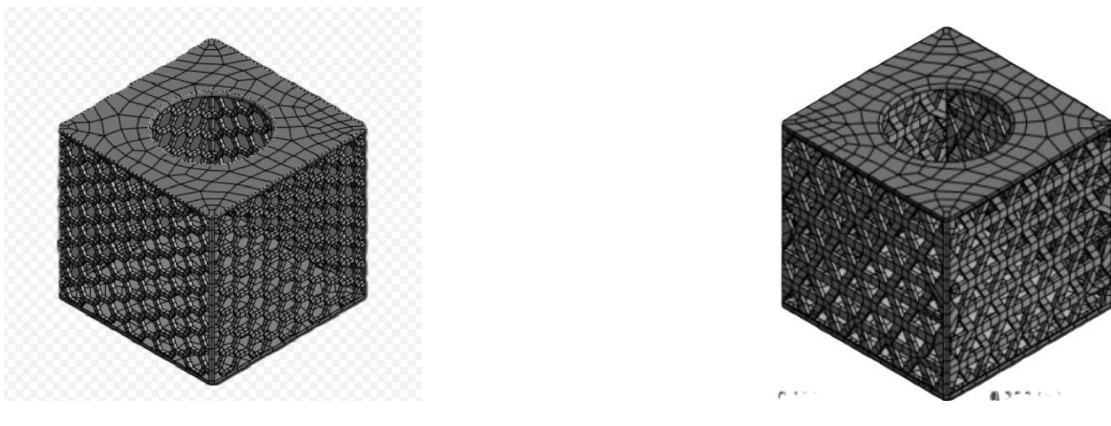
131 The analysis utilized the material properties of Aluminium 6061-T6, a standard aerospace-grade alloy. The
132 mechanical input parameters are summarised in **Table 2**.

133 **Table 2:** Mechanical input parameters

Property	Value	Unit
Yield Strength	276	MPa
Modulus of Elasticity	68.9	GPa
Poisson's Ratio	0.33	dimensionless

134

135



136

137 (a)

(b)

138 **Figure 2.1:** Small Satellite Structure with (a) honeycomb body panel and (b) with iso-grid body panel

139

140



141

142

Figure 2.2: Small satellite structure used for FEA analysis and 3D printing

143 **2.3 Additive Manufacturing**

144 The Structure was printed in the Additive Manufacturing lab(G07) in GD Naidu block, VIT , Vellore, using the
145 QIDI X-MAX3 Machine as illustrated in **Figure. 2.3** . The material used was PLA (polylactic acid) for the
146 prototype. It was a polymer-based prototype and it demonstrated an actual 3d printed material along a support
147 structure required in the printing process.



148

149

Figure 2.3 : QIDI X-MAX3 3d printing machine

150

151 **3 Results and Discussion**

152 **3.1 Product design and Analysis**

153 The structural performance of the satellite frame was analysed using Ansys 2025R1 Student Version, with a focus
154 on static structural analysis.

155 The boundary conditions applied in the simulation included fixed constraints at the mounting points and external
156 forces to simulate launch loads. The forces were applied in accordance with industry standards for satellite
157 launches, considering both gravitational and vibrational forces during lift-off. The simulations aimed to ensure
158 that the satellite structure could withstand the loads without exceeding the material's yield strength.

159 The material properties of Aluminium 6061-T6 were input into the simulation, including its yield strength (276
160 MPa), modulus of elasticity (68.9 GPa), and Poisson's ratio (0.33). The analysis confirmed that the structure had
161 a sufficient safety margin, with stress levels well below the yield point of the material.

162 The static structural analysis performed in SolidWorks provided valuable insights into the behaviour of the small
163 satellite structure under the defined load conditions. The key results from the simulation are as follows:

164 *Von Mises Stress*: The stress analysis revealed that the Von Mises stress across the structure ranged from $1.021 \times$
165 10^2 N/m² to 9.804×10^7 N/m². The highest stress occurred in areas with concentrated loads but remained
166 significantly below the yield strength of aluminium 6061-T6 (276 MPa). This indicates that the structure will not
167 undergo plastic deformation or failure under the applied forces.

168 *Resultant Displacement*: The maximum displacement recorded was 0.1521 mm, a minimal value demonstrating
169 that the structure retains its shape and integrity during launch and operation, even under substantial external forces.

170 *Equivalent Strain*: The equivalent strain varied between 1.778×10^{-9} and 6.406×10^{-4} , showing controlled and
171 minimal deformation. This confirms that the strain remains well within acceptable limits, ensuring material
172 reliability.

173 *Factor of Safety (FOS)*: The factor of safety ranged from 2.805 (minimum) to 2.695×10^6 (maximum). With the
174 minimum FOS exceeding 2, the design is considered highly robust and capable of withstanding more than double
175 the applied loads without risk of failure, ensuring operational reliability.

176 One of the primary objectives of this study was to reduce the satellite structure's weight while preserving its
177 structural strength. By incorporating lattice structures and utilizing topology optimization, the total weight was
178 decreased from 300 g to 240 g, achieving a 20% reduction. This weight savings is crucial in aerospace
179 applications, where minimizing mass leads to lower launch costs and improved payload efficiency. The integration
180 of lattice structures in non-critical load regions effectively reduced material usage without compromising overall
181 structural performance. This contributes to both cost-effectiveness and compliance with strict lightweighting
182 requirements in the space industry.

183 The final design successfully met all load-bearing and performance criteria. Simulation results confirmed that
184 both von Mises stress and deformation remained well within safe limits, verifying the structure's ability to endure
185 the stresses experienced during launch, including axial loads, vibrations, and other mechanical forces.
186 Additionally, the high factor of safety further highlights the reliability of the design, indicating intentional
187 overengineering for added security.

188 The design was tailored for manufacturing through laser bed 3D metal printing, specifically using the Selective
189 Laser Melting (SLM) process. The simulation and optimization process ensured that the structure could be
190 fabricated in three separate parts, preserving the intricate lattice geometries while simplifying production. This
191 partitioned approach minimizes manufacturing complexity, reduces the need for support structures, shortens build
192 time, and cuts material waste, making the process both time- and cost-efficient.

193 The materials considered for this project included aluminium 6061-T6 and AlSi10Mg. aluminium 6061-T6 was
194 selected due to its excellent strength-to-weight ratio and compatibility with additive manufacturing. On the other

195 hand, AlSi10Mg, commonly favoured in industrial-level additive manufacturing, offers superior mechanical
196 properties, including better flow characteristics during printing and higher tensile strength. While aluminium
197 6061-T6 was primarily used in this study due to its availability and mechanical performance, AlSi10Mg may offer
198 additional advantages in terms of thermal stability and print quality in future applications.

199 Further, **Table 3** highlights the key properties of the small satellite structure considered for the study.

200 **Table 3:** Meshed Small Satellite Structure

Document name and reference	Treated As	Volumetric properties
Small Satellite Structure	Solid Body	Mass: 0.0931576
		Volume: 3.45028e-05 m ³
		Density: 2,700 kg/m ³
		Weight: 0.0912944N

201 **Table 4** highlights the boundary conditions considered for the study.

202 **Table 4:** Boundary conditions used in the study

Parameters	Options Selected
Analysis type	Static
Mesh type	Solid mesh
Thermal effect	On
Thermal option	Include temperature tools
Zero strain temperature	298 Kelvin
Solver Type	Automatic
In plane Effect	Off
Soft Spring	Off
Inertial Relief	Off
Incompatible Bonding Options	Automatic
Large Displacements	Off
Compute Free Body Forces	On
Friction	Off
Use Adaptive Method	Off

203 **Table 5** highlights the materials properties considered for the study.

204 **Table 5:** Material Properties

Model Reference	Properties	Value
	Yield Strength	2.75e+08 N/m ²
	Tensile Strength	3.1e+08 N/m ²
	Elastic Modulus	6.9e+10 N/m ²
	Poisson's Ratio	0.33
	Mass Density	2700 kg/m ³
	Shear Modulus	2.6e+10 N/m ²
	Thermal Expansion Coefficient	2.4e-05 /Kelvin

205

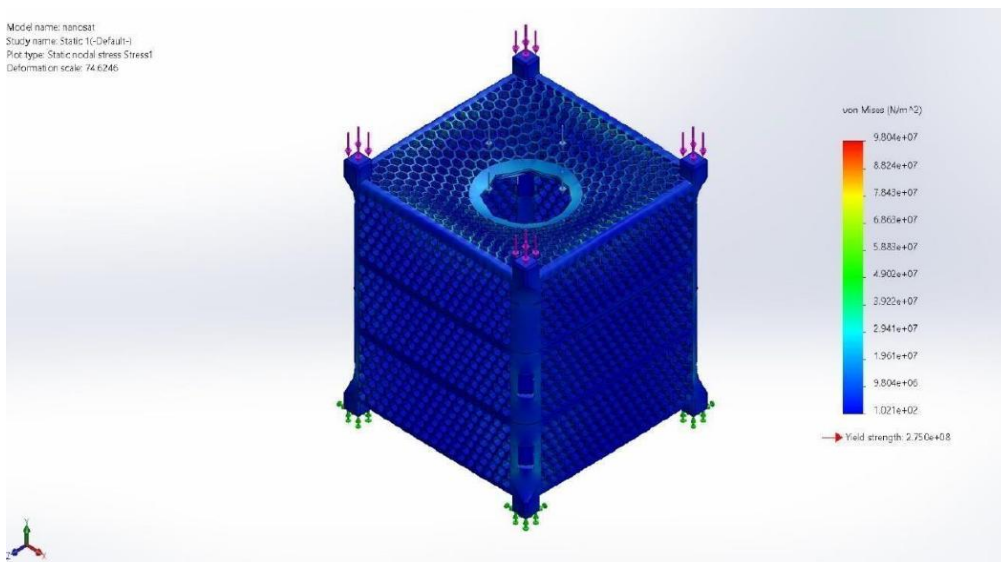
206 The structural integrity of the developed satellite system was rigorously evaluated using key criteria derived from
207 Finite Element Analysis (FEA), specifically the Von Mises stress, resultant displacement, equivalent strain, and
208 the corresponding Factor of Safety (FOS). The results presented below elucidate the system's mechanical
209 performance under simulated load conditions.

210 Von Mises stress is the primary criterion used to assess the likelihood of material yielding under complex, multi-
211 axial loading. The minimum nodal stress recorded was 1.021×10^2 N/m². This low value is consistent with regions
212 near free or unconstrained boundaries that are subjected to negligible loading. The peak stress concentration was
213 observed at Node 91026, registering 9.804×10^7 N/m². This location merits close examination to confirm that the
214 observed stress remains comfortably below the material's yield strength. The overall nodal stress distribution is
215 visually represented in **Figure 3.1**.

216 Resultant Displacement (URES) quantifies the total structural movement induced by the applied load, as depicted
217 in **Figure 3.2**. A minimum displacement of 0.000 mm was recorded at Node 59599. This finding is consistent with
218 the fixed or constrained anchoring boundary conditions applied at this node in the simulation. The maximum
219 displacement was found to be 0.1521 mm at Node 100455. The extremely small magnitude of this peak
220 displacement (significantly below 1 mm) confirms the structure's satisfactory stiffness and integrity under the
221 simulated load. The complete displacement field is presented in **Figure 3.2**.

222 Equivalent Strain (ESTRN) provides a composite measure of structural deformation and change in shape. As
223 shown in **Figure 3.3**, the strain field analysis yielded the following results. The minimum strain recorded was
224 1.778×10^{-9} in Element 83487, reflecting non-deformed or rigid structural regions. The maximum strain was
225 found to be -6.406×10^{-4} in Element 49009. This element typically corresponds to domains subject to pronounced
226 bending or sections carrying the highest load. The distribution and regions of notable strain are visualized in
227 **Figure 3.3**.

228 Safety margins are a pivotal metric in aerospace engineering, and the Factor of Safety (FOS) quantifies the strength
229 margin beyond the applied operational loads. The FOS results are mapped in **Figure 3.4**. The minimum observed
230 FOS of 2.805 occurred at Node 91026, which coincides with the location of maximum Von Mises stress. This
231 margin is deemed acceptable for aerospace applications, where standards generally require FOS values above 2.0
232 for critical components. The maximum FOS was 2.695×10^6 at Node 253438. This extremely high value is
233 expected in underloaded regions that are removed from major stress paths. Additionally, the Fatigue Assessment,
234 presented in **Figure 3.5**, supports the static evaluation by providing insights into the structure's long-term
235 durability under anticipated cyclic loading scenarios.

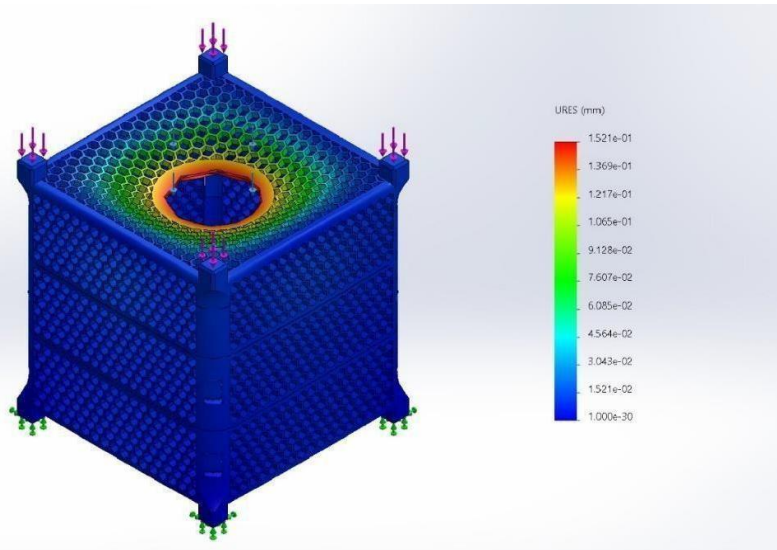


236

237

Figure 3.1: Static Nodal Stress

Model name: nanosat
Study name: Static 1 (Default)
Plot type: Static displacement, Displacement1
Deformation scale: 74.6246



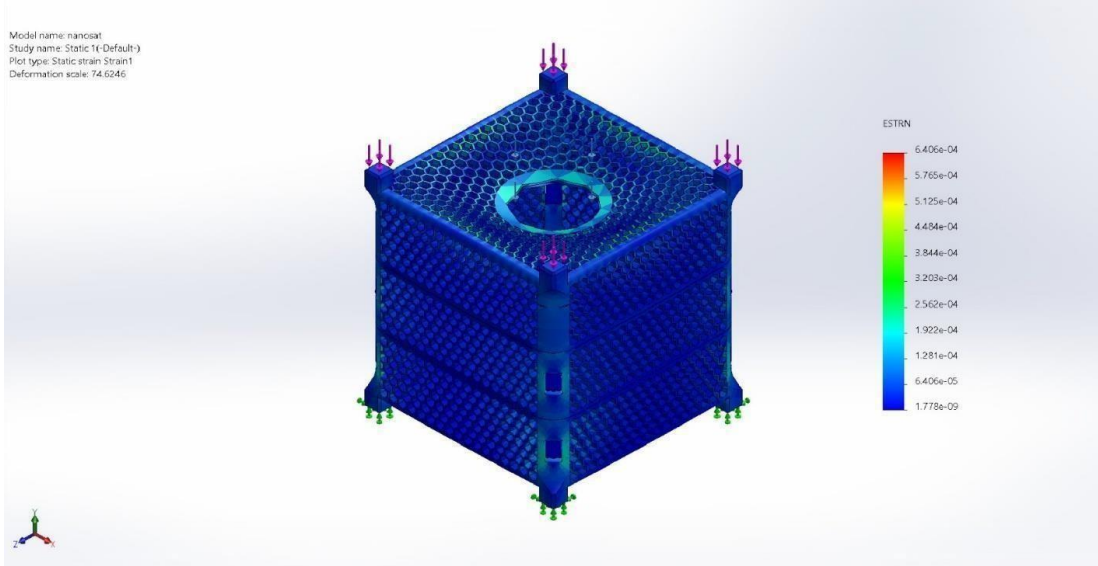
238

239

240

241

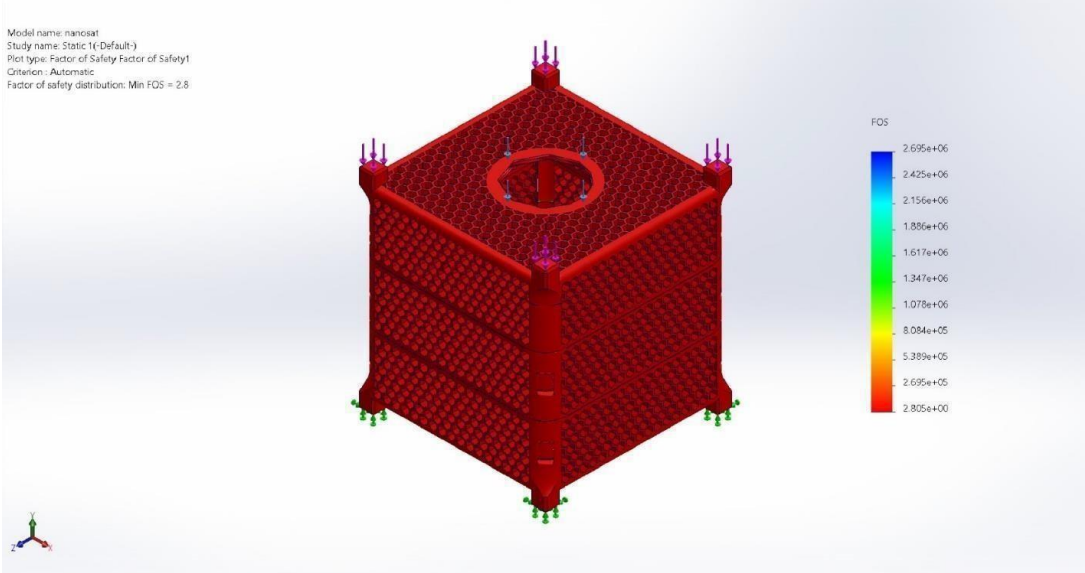
Figure 3.2: Static Displacement



242

243

Figure 3.3: Static Strain



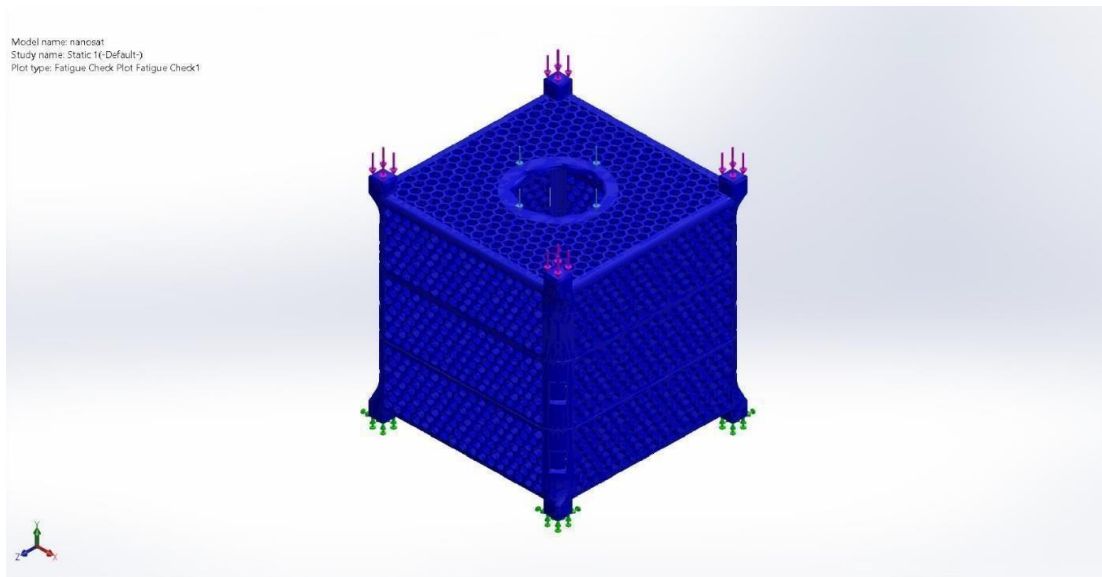
244

245

246

247

Figure 3.4: Factor of Safety



248

249

250 **Table 6** summarizes the minimum and maximum results per metric for clarity.

251 **Table 6:** Minimum and maximum results of simulation study

Metric	Type	Minimum (Location)	Maximum (Location)
Static Nodal Stress	Von Mises Stress	$1.021 \times 10^2 \text{ N/m}^2$ (Node: 253438)	$9.804 \times 10^7 \text{ N/m}^2$ (Node: 91026)
Displacement	Resultant (URES)	0.0 mm (Node: 59599)	0.1521 mm

			(Node: 100455)
Strain	Equivalent (ESTRN)	1.778×10^{-9} (Element: 83487)	-6.406×10^{-4} (Element: 49009)
Factor of Safety	Automatic	2.805 (Node: 91026)	2.695×10^6 (Node: 253438)

252

253 **3.2 Additive Manufacturing Process**

254 The final design was tailored for manufacturing through fused deposition modelling. The simulation and
255 optimization process ensured that the structure could be fabricated in three separate parts, preserving the intricate
256 lattice geometries while simplifying production. This partitioned approach minimizes manufacturing complexity,
257 reduces the need for support structures, shortens build time, and cuts material waste, making the process both
258 time- and cost-efficient.

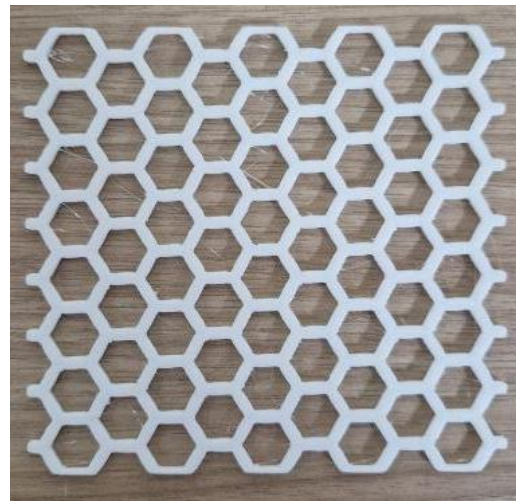
259 The prototype model of the satellite structure was produced using Fused Deposition Modelling (FDM) with
260 Polylactic Acid (PLA) as the primary material. This approach allowed for rapid and cost-effective prototyping
261 before committing to metal-based manufacturing. The prototype was fabricated in the additive manufacturing lab
262 located in the G.D. Naidu block, utilizing the QIDI X-MAX3 3D printing machine. This step was essential for
263 verifying form, fit, and assembly aspects of the design prior to final production.

264 For real-time production, the selected material is aluminium alloy, which offers superior strength and durability
265 under operational conditions. The use of aluminium in combination with advanced additive manufacturing
266 techniques like SLM ensures that the final product will meet the stringent requirements of space applications.
267 Additionally, the project considered the use of AlSi10Mg, an aluminium alloy commonly employed in industrial
268 additive manufacturing, due to its excellent mechanical properties, better printability, and enhanced thermal
269 stability. AlSi10Mg may be particularly useful in future iterations of the design, especially where high precision
270 and thermal performance are critical.



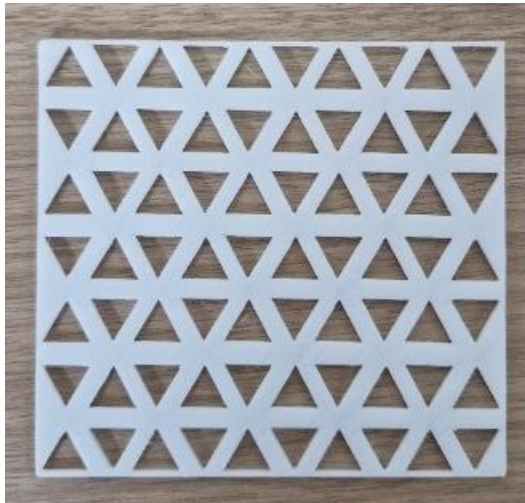
271

272 **Figure 3.6:** 3D printed base part



273 **Figure 3.7:** 3D printed honeycomb panel

274



275

276

Figure 3.8: 3D printed iso-grid panel**Figure 3.9:** 3D printed sidebar

277

278

Figure 3.10: 3D printed top part**Figure 3.11:** 3D printed small satellite structure

279

All these structures were printed with a total time taken around 38-40 hrs. The satellite structure took 18 hrs to complete while the other structures took around 4 hrs to complete each part. Detailed description about time taken to print each component is mentioned in **Table 7**.

280

Table 7: Time taken to print each component

Name of the part	Time Taken
Side bar	10 mins
Base	4 hrs
Top	5 hrs
Honeycomb panel	5 hrs
Isogrid panel	5 hrs

281

The Table 7 outlines the estimated or recorded time spent on manufacturing or assembling key components of satellite structure. Each row corresponds to a specific part, along with the time taken to either fabricate or integrate it into the complete system.

286 Side bar (10 minutes): The side bar is a relatively simple structural component, likely fabricated quickly due to
287 its small size or straightforward geometry. This short time suggests minimal complexity, possibly a standard part
288 made using rapid techniques like laser cutting or 3D printing.

289 Base (4 hours): The base forms a foundational component of the satellite, providing structural support for the rest
290 of the system. The 4-hour duration reflects the need for precision and perhaps more robust materials or multiple
291 sub-assemblies.

292 Top (5hours): Like the base, the top part of the satellite requires careful fabrication, especially if it supports
293 antennas, solar panels, or deployment mechanisms. The slight increase in time may indicate added complexity in
294 geometry or integration with other subsystems.

295 Honeycomb panel (5 hours) : The honeycomb panel is likely a structural or protective component used for strength
296 and lightweighting. Its fabrication involves careful layering or bonding processes, which justifies the time spent.
297 The consistent 5-hour timeframe with other panels shows a standard fabrication effort for such advanced
298 structures.

299 Iso-grid panel(5 hours): Like the honeycomb panel, the isogrid panel is a lightweight structural component
300 designed for stiffness and strength. Fabricating iso-grid structures may involve complex machining or 3D printing
301 with internal patterns, accounting for the identical time spent as the honeycomb panel.

302 Satellite(18 hours): This represents the total time required to assemble all components, integrate subsystems,
303 perform fit checks, and possibly preliminary testing. It is significantly longer than the time for individual parts,
304 highlighting the complexity of full satellite integration and the attention to detail needed to ensure structural and
305 functional reliability.

306 **4. Conclusions**

307 The design and development of the small satellite structure highlighted the effectiveness of integrating advanced
308 engineering techniques, such as topology optimization and lattice structure integration, to achieve significant
309 weight reduction while maintaining the necessary structural integrity. These modern design approaches allowed
310 for the efficient distribution of material, ensuring that strength was retained only where needed, ultimately
311 contributing to an optimized and lightweight design suitable for space applications. Static analysis, conducted
312 using Ansys R12025 Student Version, played a crucial role in evaluating the structural performance of the satellite
313 under various load conditions typically encountered during launch and orbital operation. The boundary conditions
314 applied in the simulation included fixed constraints at the mounting points and external forces to simulate launch
315 loads. The forces were applied in accordance with industry standards for satellite launches, considering both
316 gravitational and vibrational forces during lift-off. The simulations aimed to ensure that the satellite structure
317 could withstand the loads without exceeding the material's yield strength.

318 The material properties of Aluminium 6061-T6 were input into the simulation, including its yield strength (276
319 MPa), modulus of elasticity (68.9 GPa), and Poisson's ratio (0.33). The analysis confirmed that the structure had
320 a sufficient safety margin, with stress levels well below the yield point of the material. The static structural analysis
321 performed in SolidWorks provided valuable insights into the behaviour of the small satellite structure under the
322 defined load conditions.

323 The stress analysis revealed that the Von Mises stress across the structure ranged from 1.021×10^2 N/m² to 9.804×10^7 N/m². The highest stress occurred in areas with concentrated loads but remained significantly below the
324 yield strength of aluminium 6061-T6 (276 MPa). This indicates that the structure will not undergo plastic
325 deformation or failure under the applied forces. The maximum displacement recorded was 0.1521 mm, a minimal
326 value demonstrating that the structure retains its shape and integrity during launch and operation, even under
327 substantial external forces. The equivalent strain varied between 1.778×10^{-9} and 6.406×10^{-4} , showing controlled
328 and minimal deformation. This confirms that the strain remains well within acceptable limits, ensuring material
329 reliability. The factor of safety ranged from 2.805 (minimum) to 2.695×10^6 (maximum). With the minimum FOS
330 exceeding 2, the design is considered highly robust and capable of withstanding more than double the applied
331 loads without risk of failure, ensuring operational reliability.

333 One of the primary objectives of this project was to reduce the satellite structure's weight while preserving its
334 structural strength. By incorporating lattice structures and utilizing topology optimization, the total weight was
335 decreased. This weight savings is crucial in aerospace applications, where minimizing mass leads to lower launch
336 costs and improved payload efficiency. The integration of lattice structures in non-critical load regions effectively
337 reduced material usage without compromising overall structural performance. This contributes to both cost-
338 effectiveness and compliance with strict lightweighting requirements in the space industry.

339 The final design was tailored for manufacturing through fused deposition modelling. The simulation and
340 optimization process ensured that the structure could be fabricated in three separate parts, preserving the intricate
341 lattice geometries while simplifying production. This partitioned approach minimizes manufacturing complexity,
342 reduces the need for support structures, shortens build time, and cuts material waste, making the process both
343 time- and cost-efficient.

344 The materials considered for this project included aluminium 6061-T6 and AlSi10Mg. Aluminium 6061-T6 was
345 selected due to its excellent strength-to-weight ratio and compatibility with additive manufacturing. On the other
346 hand, AlSi10Mg, commonly favoured in industrial-level additive manufacturing, offers superior mechanical
347 properties, including better flow characteristics during printing and higher tensile strength. While Aluminium
348 6061-T6 was primarily used in this study due to its availability and mechanical performance. AlSi10Mg may offer
349 additional advantages in terms of thermal stability and print quality in future applications.

350 The successful deployment and operation of small satellites heavily depend on the efficiency of their structural
351 systems. By focusing on optimizing mass-to-strength ratios, enhancing modularity, adopting additive
352 manufacturing, and addressing challenges related to subsystem integration, thermal management, and
353 sustainability, engineers can significantly improve the performance, reliability, and affordability of small satellite
354 missions. The continuous evolution of structural materials and design methodologies will further open new
355 frontiers in small satellite engineering, ensuring this compact spacecraft play a pivotal role in the future of space
356 exploration and utilization.

357 References

- 358 Boudjemai, A., Bouanane, M. H., Merad, L., & Mohammed, A. S. (2007, June). Small satellite structural
359 optimisation using genetic algorithm approach. In 2007 3rd International Conference on Recent Advances in
360 Space Technologies (pp. 398-406). IEEE. DOI: 10.1109/RAST.2007.4284021
- 361 Becedas, J., & Caparrós, A. (2018). Additive manufacturing applied to the design of small satellite structure for
362 space debris reduction. Applications of Design for Manufacturing and Assembly, 59-76. DOI:
363 10.5772/intechopen.78762
- 364 Aborehab, A., Kassem, M., Nemnem, A. F., & Kamel, M. (2023). Structural optimization of a small earth remote
365 sensing satellite. Noise & Vibration Worldwide, 54(10-11), 539-556. <https://doi.org/10.1177/09574565231203252>
- 366 Boudjemai, Abdelmadjid & Bekhti, M. & Bouanane, Mohamed El Houari & Mohammed, A. & Cooper, G. &
367 Richardson, Guy. (2005). Small satellite computer-aided design and manufacturing. 581. 36.
- 368 Ganga, P. L., Micheletti, A., Podio-Guidugli, P., Scolamiero, L., Tibert, G., & Zolesi, V. (2016). Tensegrity rings
369 for deployable space antennas: concept, design, analysis, and prototype testing. Variational analysis and aerospace
370 engineering: Mathematical challenges for the aerospace of the future, 269-304. DOI: 10.2140/jomms.2007.2.857
- 371 Colas, F., Zanda, B., Bouley, S., Jeanne, S., Malgoyre, A., Birlan, M., ... & Dardon, A. (2020). FRIPON: a
372 worldwide network to track incoming meteoroids. Astronomy & Astrophysics, 644, A53.
373 <https://doi.org/10.1051/0004-6361/202038649>

374